PHYSICAL REVIEW B, VOLUME 65, 201102(R)

Light scattering from a monolayer of periodically arrayed dielectric spheres on dielectric substrates

Y. Kurokawa and H. Miyazaki*
Department of Applied Physics, Tohoku University, Aramaki, Aoba, Sendai 980-8579, Japan

Y. Jimba
College of Engineering, Nihon University, Koriyama, Fukushima 963-8642, Japan
(Received 6 February 2002; published 8 May 2002)

Theoretical studies have revealed that coupling with a dielectric substrate significantly affects the transmission spectrum of a 2D photonic crystal of monolayer dielectric spheres. The dielectric constant of a semi-infinite substrate has been found to have a threshold, above which dips in the transmission spectrum broaden drastically. A substrate of finite thickness yields additional dips in the spectrum corresponding to localized eigenstates within the substrate. The transmission spectrum is well explained by the anticrossing of the eigenstates of a monolayer and a substrate.

DOI: 10.1103/PhysRevB.65.201102 PACS number(s): 42.70.Qs, 42.25.Bs, 42.79.−e

Research on photonic crystals[1] (PC's) has been focused for many years on the realization of a complete-gap PC, i.e., a PC having a common photonic gap in all directions. A complete-gap PC could be used, for example, in fundamental QED experiments to control the atomic lifetime by the suppression of spontaneous emission.[2] A variety of possible complete-gap PC's have been found in theoretical studies.[3] Since gaps appear as a result of interference, long-range order in all directions is indispensable for three-dimensional (3D) PC's. To realize complete-gap PC's, therefore, highly sophisticated methods such as self-assembly or autocloning[4] have been developed in addition to the advanced technology of lithography.[5] At present, however, it is still difficult to obtain 3D PC's of high quality.

In contrast, 2D slablike PC's with long-range order,[6] a typical example being a monolayer of periodically arrayed dielectric spheres on a substrate, can easily be fabricated. Many theoretical[7] and experimental[8–10] studies on the transmission spectra and photonic band structures of such PC's are currently being carried out. A slablike PC is different from ordinary 2D PC's composed of infinitely long parallel cylinders, in that it has a finite thickness in one direction. Consequently, there is an energy dissipation in that direction, which gives rise to a finite lifetime of its eigenstates. There is also a significant enhancement of the electric field near the surface (near field) by diffracted evanescent waves due to the 2D periodicity.[7] This enhancement can be observed by the use of a scanning near-field optical microscope.[11] There is, in fact, a strong demand for the development of new photon technology by utilizing enhanced near fields such as laser manipulation of atoms.[12]

The relevant wavelength of a slab-type PC at present is comparable with the 2D periodicity. For example, it lies in the lower Mie resonance region ($l \cong 3,4$) for monolayer spheres.[13] An electric field of such lower resonances is not strongly localized within the spheres and leaks out of the monolayer. This extended nature of the electric field is expected to induce strong coupling with the substrate. However, this coupling was not taken into account in our previous study.[7] A few theoretical attempts[14] have been made to analyze the optical properties of a 2D periodic system on a semi-infinite substrate, but all of them lack the viewpoint of PC's such as band structure. There has been no theoretical study on the effect of a substrate of finite thickness.

In this study we extend our previous theory[7] and investigate the effect of a dielectric substrate on the transmission spectrum of a monolayer of periodically arrayed dielectric spheres. We found that the substrate dramatically changes the transmission spectrum of the monolayer spheres. Our results show that the optical properties of monolayer spheres can be easily controlled by choosing an appropriate dielectric substrate.

We deal with the following monolayer spheres on a substrate (see inset in Fig. 1). The spheres have a common radius a and a uniform dielectric constant ϵ_Q and form a close-packed triangular lattice. The substrate has a uniform

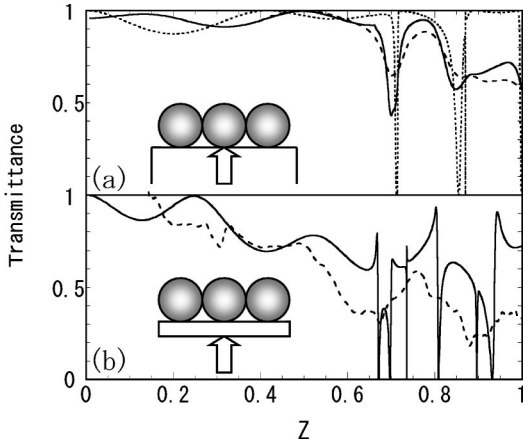

FIG. 1. Transmission spectra of a monolayer of periodically arrayed dielectric spheres on (a) a semi-infinite substrate and (b) a finite substrate for perpendicular incidence. Parameters are (a) $\epsilon_Q = 2.56$, $a = 490$ nm, $\epsilon_S = 2.28$ and (b) $\epsilon_Q = 2.56$, $a = 1$ μm, $\epsilon_S = 4.41$, $d = 0.3$ μm. Solid and broken lines show the calculated and experimental results,[8,10] respectively. The dotted line in (a) shows the results in the case of a monolayer without a substrate. The configuration used in each case is shown in the inset.

dielectric constant ϵ_S and is either semi-infinite or has a thickness d. The origin of the coordinates is at the center of one of the spheres. The xy plane is set parallel to the surface of the substrate and the x axis penetrates the origins of the spheres in contact. The substrate occupies the negative z region. Light velocity c in the vacuum is taken to be unity.

Let us first consider the scattering from monolayer spheres alone. When a plane electromagnetic wave $\mathbf{E}(\mathbf{r}) = \mathbf{E}^0 \exp(i\mathbf{k}_0 \cdot \mathbf{r})$ is incident from $z<0$ with the wave vector $\mathbf{k}_0 = (\mathbf{k}_\parallel, k_z)$, it is multiply scattered within the monolayer and finally emerges from the monolayer as plane waves with the in-plane wave vector $\mathbf{k}_\parallel + \mathbf{h}$. Here, $\mathbf{h}$ is a 2D reciprocal lattice vector acquired by umklapp scattering. Thus, the scattered wave is a sum of plane waves with wave vectors $\mathbf{k}_\mathbf{h}^\pm = (\mathbf{k}_\parallel + \mathbf{h}, \Gamma_\mathbf{h}^\pm)$, where $\Gamma_\mathbf{h}^\pm$ is given by energy conservation as $\Gamma_\mathbf{h}^\pm = \pm\sqrt{\mathbf{k}_0^2 - (\mathbf{k}_\parallel + \mathbf{h})^2}$:

$$\mathbf{E}_i(\mathbf{r}) = \begin{cases} \sum_{\mathbf{h},j} T_Q(i,\mathbf{h};j,\mathbf{0}) \exp(i\mathbf{k}_\mathbf{h}^+ \cdot \mathbf{r}) E_j^0, & z > a \\ \sum_{\mathbf{h},j} R_Q(i,\mathbf{h};j,\mathbf{0}) \exp(i\mathbf{k}_\mathbf{h}^- \cdot \mathbf{r}) E_j^0, & z < -a. \end{cases} \tag{1}$$

Here, $T_Q(i,\mathbf{h};j,\mathbf{h}')$ and $R_Q(i,\mathbf{h};j,\mathbf{h}')$ are obtained by expanding the incident and scattered waves in terms of vector spherical harmonics and by incorporating the multiple intrasphere and intersphere scattering within the monolayer.[7]

A semi-infinite substrate is taken into account by the interface matrices, which relate the incident, reflected, and transmitted waves $\mathbf{E}^{inc}$, $\mathbf{E}^{ref}$, and $\mathbf{E}^{trans}$ at the substrate surface:

$$(\mathbf{E}^{trans})_i = \sum_j T_S(i,j;\mathbf{h},\epsilon_0,\epsilon_S)(\mathbf{E}^{inc})_j, \tag{2a}$$

$$(\mathbf{E}^{ref})_i = \sum_j R_S(i,j;\mathbf{h},\epsilon_0,\epsilon_S)(\mathbf{E}^{inc})_j. \tag{2b}$$

Note that wave vectors of reflected and transmitted waves are given by $\mathbf{k}_\mathbf{h}^+ = (\mathbf{k}_\parallel + \mathbf{h}, \Gamma_\mathbf{h}^+)$ and $\mathbf{q}_\mathbf{h}^- = (\mathbf{k}_\parallel + \mathbf{h}, \gamma_\mathbf{h}^-)$, respectively, for an incident wave of $\mathbf{k}_\mathbf{h}^- = (\mathbf{k}_\parallel + \mathbf{h}, \Gamma_\mathbf{h}^-)$. Here, $\gamma_\mathbf{h}^\pm$ is given by $\pm\sqrt{(\epsilon_S - 1)(\mathbf{k}_\parallel + \mathbf{h})^2 + \epsilon_S(\Gamma_\mathbf{h}^-)^2}$. Boundary conditions at the substrate surface give $T_S(i,j;\mathbf{h},\epsilon_0,\epsilon_S)$ as

$$T_S(\mathbf{h},\epsilon_0,\epsilon_S) = \begin{pmatrix} \frac{2\Gamma_\mathbf{h}^-}{\Gamma_\mathbf{h}^- + \gamma_\mathbf{h}^-} & 0 & \frac{2\Gamma_\mathbf{h}^-(\epsilon_0 - \epsilon_S)(\mathbf{k}_\parallel + \mathbf{h})_x}{(\Gamma_\mathbf{h}^- \epsilon_S + \gamma_\mathbf{h}^- \epsilon_0)(\Gamma_\mathbf{h}^- + \gamma_\mathbf{h}^-)} \\ 0 & \frac{2\Gamma_\mathbf{h}^-}{\Gamma_\mathbf{h}^- + \gamma_\mathbf{h}^-} & \frac{2\Gamma_\mathbf{h}^-(\epsilon_0 - \epsilon_S)(\mathbf{k}_\parallel + \mathbf{h})_y}{(\Gamma_\mathbf{h}^- \epsilon_S + \gamma_\mathbf{h}^- \epsilon_0)(\Gamma_\mathbf{h}^- + \gamma_\mathbf{h}^-)} \\ 0 & 0 & \frac{2\Gamma_\mathbf{h}^- \epsilon_0}{\Gamma_\mathbf{h}^- \epsilon_S + \gamma_\mathbf{h}^- \epsilon_0} \end{pmatrix}. \tag{3}$$

$R_S(i,j;\mathbf{h},\epsilon_0,\epsilon_S)$ is obtained by replacing the numerator of diagonal elements in $T_S(i,j;\mathbf{h},\epsilon_0,\epsilon_S)$ as $2\Gamma_\mathbf{h}^- \to \Gamma_\mathbf{h}^- - \gamma_\mathbf{h}^-$ and $2\Gamma_\mathbf{h}^- \epsilon_0 \to \Gamma_\mathbf{h}^- \epsilon_S - \gamma_\mathbf{h}^- \epsilon_0$.

For a substrate of finite thickness d, we use the propagation matrix within the substrate $P(\mathbf{h},\epsilon_S) = \exp(i\gamma_\mathbf{h}^+ d) I$, where I is a 3×3 unit matrix. Interface matrices for an incident wave from the inner side of the substrate are obtained by replacing $\Gamma_\mathbf{h}^- \leftrightarrow \gamma_\mathbf{h}^+$ and $\epsilon_0 \leftrightarrow \epsilon_S$ in $T_S(i,j;\mathbf{h},\epsilon_0,\epsilon_S)$ and $R_S(i,j;\mathbf{h},\epsilon_0,\epsilon_S)$. A combination of these matrices gives the transmission and reflection matrices for a semi-infinite or finite substrate. Finally, the multiple scattering between a monolayer and substrate is incorporated by the bilayer method.[15]

The transmission spectrum is calculated from the z component of the Poynting vector[7] as

$$T = \sum_\mathbf{h}{}' \left(\sum_i \left| \sum_j \hat{T}(i,\mathbf{h};j,\mathbf{0}) E_j^0 \right|^2 \right) \cos(\hat{\mathbf{k}}_\mathbf{h}^+ \cdot \hat{\mathbf{z}}). \tag{4}$$

Here, $\hat{T}(i,\mathbf{h};j,\mathbf{0})$ gives the amplitude of plane waves above the monolayer when a plane wave of unit amplitude and wave vector $\mathbf{k}_0$ is incident upon the system. Vectors with carets are unit vectors. The scattering channel specified by $\mathbf{h}$ is called open (closed) when $\Gamma_\mathbf{h}^\pm$ is real (imaginary). Only open channels contribute to the transmission spectrum, while closed channels enhance the near field. Primed summation means the sum only over open channels. Since only the main channel ($\mathbf{h}=\mathbf{0}$) is observed in experiments, we focus on this channel hereafter.

To study the effect of the substrate and to clarify the underlying physics, it is sufficient to deal only with the perpendicular incidence. Transmission for oblique incidence gives information on the photonic band structure. Owing to the scaling rule,[1] we need only to calculate the transmission as a function of the dimensionless parameter $Z = \sqrt{3}a/\lambda$, where λ is a wavelength. A triangular lattice has six nonzero smallest $\mathbf{h}$'s. These are called the first shell and correspond to $Z=1$. Below $Z=1$, therefore, only the main channel ($\mathbf{h}=\mathbf{0}$) gives the propagating wave, and all other channels are evanescent. Since a rich structure for $Z \leqslant 1$ has been found in experiments, we focus on this region in the present paper. Suffi-

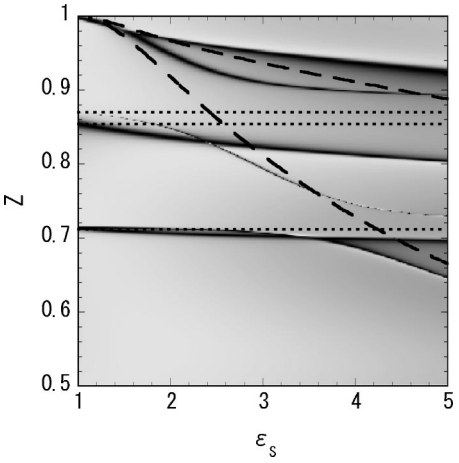

FIG. 2. Transmission spectra of monolayers on finite substrates of $d=0.3$ μm, $0.5\leqslant Z\leqslant 1$, and $1\leqslant\epsilon_S\leqslant 5$. The darker region corresponds to lower transmission. Horizontal dotted lines show the dip positions without a substrate. The two downward broken curves from $Z=1$, $\epsilon_S=1$ are solutions of Eq. (5).

cient numerical convergence is attained for $Z\leqslant 1$ by expanding the vector spherical harmonics up to $l_{max}=9$ and including reciprocal lattice vectors of the third shell (18 nonzero $\mathbf{h}$'s).

Solid lines in Figs. 1(a) and 1(b) show the calculated transmission spectra of monolayer polystyrene spheres ($\epsilon_Q=2.56$) on (a) a semi-infinite substrate ($\epsilon_S=2.28$) and (b) a SiN substrate of finite thicknesses ($\epsilon_S=4.41, d=0.3$ μm). The radii of the spheres are (a) $a=490$ nm and (b) $a=1$ μm. The dotted line in Fig. 1(a) is the transmission spectrum without a substrate. The broken lines in Fig. 1 show the experimental results.[8,10] In the experiment on a finite substrate, 91 spheres were arranged in a triangular lattice using a micromanipulation system.

Transmission without a substrate has sharp dips at $Z=0.712$, 0.854, and 0.870. Dips at $Z=0.712$ are almost degenerate. As seen in Fig. 1(a), a semi-infinite substrate broadens and shifts the dips at $Z=0.712$ to $Z\cong 0.70$. Dips at $Z=0.854$ and 0.870 merge into a broad dip near $Z=0.85$. Inclusion of a semi-infinite substrate reproduces the characteristic features of the experimental results except for dip width. Dip width is thought to depend on the sample quality, and dips would thus be more sharpened for higher quality. However, our results show that even an ideal sample has a finite dip width.

Dips in the transmission spectrum represent the excitation of eigenstates of the system. Since the system is in a vacuum, there is an energy flow outside the system. This dissipation gives a finite lifetime to the eigenstates and results in the broadening of dips. The energy dissipation is brought about only by the nonevanescent transmitted and reflected waves. When the in-plane wave vector is $\mathbf{h}$ for perpendicular incidence, the z component in the vacuum is $\pm\sqrt{Z^2-\mathbf{h}^2}$. Thus, for a monolayer without a substrate, only the main channel ($\mathbf{h}=\mathbf{0}$) contributes to the broadening for $Z\leqslant 1$. When a semi-infinite substrate is present, however, the z component within the substrate changes to $\pm\sqrt{\epsilon_S Z^2-\mathbf{h}^2}$. Thus, evanescent

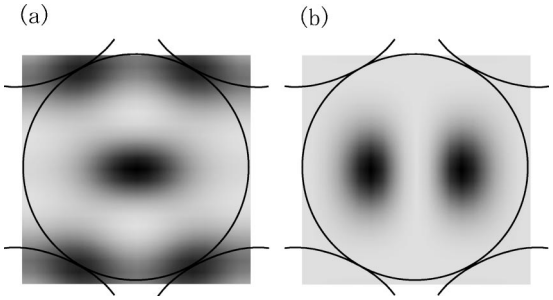

FIG. 3. Contour plots of near-field intensity at (a) $Z=0.670$ and (b) $Z=0.698$ for monolayer spheres on a finite substrate. The darker region corresponds to higher field intensity. Field variation is (a) $0.45\leqslant|\mathbf{E}|^2\leqslant 109.16$ and (b) $0.02\leqslant|\mathbf{E}|^2\leqslant 133.24$. Parameters are the same as those listed in the caption of Fig. 1(b). The sampling plane is at $z=-a$. Solid curves show the circumferences of the spheres.

waves of Z above the threshold value $Z_{th}=|\mathbf{h}|/\sqrt{\epsilon_S}$ in the vacuum are converted to propagating waves within the substrate and contribute to the energy dissipation. In other words, extra broadening of dips implies additional openings of dissipation channels through the substrate.

Conversion of evanescent waves to propagating waves in the substrate significantly affects the transmission of monolayer spheres on a substrate of finite thickness. Numerical results in Fig. 1(b) show the appearance of additional dips in addition to the complicated splitting of dips at $Z=0.712$, 0.854, and 0.870. Experimental data, on the other hand, show two broad dips at around $Z=0.65$ and 0.90 with an additional fine structure. We think that disorder of the sphere arrangement in addition to the finite size effect would smear out the fine structure of the transmission spectrum.

To determine the physical meaning of various dips shown in Fig. 1(b), we plot in Fig. 2 the transmission spectra for $0.5\leqslant Z\leqslant 1.0$ by setting d to 0.3 μm and varying the substrate dielectric constant ϵ_S. The darker region corresponds to lower transmission. We found no extra broadening of dips as in the case of a semi-infinite substrate. Rather, we observed a systematic anticrossing of dips as a function of ϵ_S. This anticrossing phenomenon seems to reflect the interaction between eigenstates of a monolayer and the substrate. Eigenstates of a monolayer are independent of ϵ_S and are shown in Fig. 2 by the horizontal dotted lines at $Z=0.712$, 0.854, and 0.870. A dielectric thin film, on the other hand, has a series of resonance states for perpendicular incidence. However, for the thickness in Figs. 1(b) or 2, the resonance is too broad to account for the sharp crossover in Fig. 2. Here, we take into account the conversion of evanescent waves in the vacuum into propagating waves within the substrate. Converted propagating waves undergo multiple total reflection from both sides of the substrate and form eigenstates localized within the substrate. The characteristic feature of these eigenstates is that they can only be excited by the evanescent waves outside the substrate. In other words, they can never be excited without the presence of 2D periodic spheres on the substrate.

To determine the validity of this idea, we calculate the change in the amplitude of the electric field for a round trip propagation within the substrate. This change is given in

terms of matrix A by $A\mathbf{E}_0$, where $\mathbf{E}_0$ is the starting amplitude. Matrix A is easily obtained by using interface and propagation matrices of the substrate. The resonance condition is given by $A\mathbf{E}_0=\mathbf{E}_0$. This yields the following equations for s- and p-polarized waves:

$$\alpha^2(\Gamma_{\mathbf{h}}^+-\gamma_{\mathbf{h}}^+)^2/(\Gamma_{\mathbf{h}}^++\gamma_{\mathbf{h}}^+)^2=1 \text{ for } s \text{ polarized,} \tag{5}$$

$$\alpha^2(\Gamma_{\mathbf{h}}^+\epsilon_S-\gamma_{\mathbf{h}}^+\epsilon_0)^2/(\Gamma_{\mathbf{h}}^+\epsilon_S+\gamma_{\mathbf{h}}^+\epsilon_0)^2=1 \text{ for } p \text{ polarized,} \tag{5}$$

where $\alpha=\exp(i\gamma_{\mathbf{h}}^+ d)$. The resonance condition requires that the evanescent wave is outside the substrate and that the propagating wave is inside the substrate. Therefore, we have $|\mathbf{h}|/\sqrt{\epsilon_S}\leqslant Z\leqslant|\mathbf{h}|$. Under this condition, $\Gamma_{\mathbf{h}}^+=i\sqrt{\mathbf{h}^2-Z^2}$ and $\gamma_{\mathbf{h}}^+=\sqrt{\epsilon_S Z^2-\mathbf{h}^2}$. Solutions of Eq. (5) are plotted in Fig. 2 by broken lines starting at $Z=1$ and $\epsilon_S=1$. From the figure, we can clearly see that the splitting of dips is a consequence of the crossover phenomenon between eigenstates of a monolayer and the substrate.

As shown in our previous paper, a huge enhancement of the near field takes place at the dip frequencies. This enhancement would also be strongly affected by the substrate. We calculate the near-field intensity distribution at each dip on the sampling square region $-a\leqslant x,y\leqslant a$. For perpendicular incidence of a p-polarized wave ($\mathbf{E}\|\hat{\mathbf{x}}$) at $Z=0.712$ without a substrate, the shape of the contour plot on the sampling plane at $z=a$ is like a lemniscate shape prolonged symmetrically along the x axis (not shown). This lemniscatelike contour reflects the field distribution of $\mathbf{E}_x$ and $\mathbf{E}_z$ having the maximum at the origin and symmetrical maxima on the x axis, respectively. The near-field intensity of a monolayer on a semi-infinite substrate at $Z=0.70$ on the same plane becomes an ellipse extending along the x axis due to the decrease in $\mathbf{E}_z$. It was also found that a semi-infinite substrate causes a reduction in the near-field intensity ($|\mathbf{E}_{max}|^2=38.3\rightarrow 6.18$).

Figures 3(a) and 3(b) show the contour plots of near fields at $Z=0.670$ and $Z=0.698$ for a substrate of finite thickness $d=0.3$ μm, respectively. The sampling plane is now located at $z=-a$. The darker region shows higher intensity. While the maximum intensities of the near fields are almost the same, their distributions are very different: the near field at $Z=0.670$ shows maxima at four contact points with the surrounding spheres in addition to the origin of the central sphere. This is due to the large y component. On the other hand, the dip at $Z=0.698$ has a large z component and shows a pair of symmetrical peaks along the x axis. We also found that the dip at $Z=0.670$ has maximum field intensity of $|\mathbf{E}_{max}|^2\cong 10^2$ within the substrate, while that at $Z=0.698$ reaches only $|\mathbf{E}_{max}|^2\cong 10$. This difference in field intensities suggests that the dips at $Z=0.670$ and $Z=0.698$ correspond to the localized eigenstates within the substrate and monolayer spheres, respectively. Details of the near-field images in addition to the photonic band structure will be reported elsewhere.

In summary, we have numerically studied the effects of semi-infinite and finite substrates on the transmission of a monolayer of periodically arrayed dielectric spheres. We found that a semi-infinite substrate significantly broadens the dips of the transmission, while a finite substrate yields additional dips in the spectrum. These findings suggest that a substrate can be used to control the optical properties of monolayer spheres. It would also be interesting to utilize the enhancement of a near field in 2D PC's by using an optically active substrate such as semiconductor quantum wells.

The authors would like to acknowledge K. Ohtaka for his valuable comments. The authors are also grateful to T. Koda, T. Itoh, Y. Segawa, T. Fujimura, H. T. Miyazaki, S. Yano, R. Shimada, and Y. Komori for a detailed explanation of the experiments. One of the authors (H.M.) expresses his gratitude to R. Okawa for his continuous encouragement and profound inspiration. This work was supported by a grant-in-aid for Scientific Research from the Ministry of Education, Science and Culture of Japan.

*Email address: hmiyazak@olive.apph.tohoku.ac.jp

[1] J.D. Joannopoulos, R.D. Meade, and J.N. Winn, *Photonic Crystals* (Princeton University Press, Princeton, 1995).

[2] A.G. Kofman, G. Kurizki, and B. Sherman, J. Mod. Opt. **41**, 353 (1994).

[3] *Photonic Band Gap Materials*, edited by C. M. Soukoulis (Kluwer, Dordrecht, 1996).

[4] S. Kawakami, Electron. Lett. **33**, 1260 (1997).

[5] C. Cuisin, A. Chelnokov, J.-M. Lourtioz, D. Decanini, and Y. Chen, Appl. Phys. Lett. **77**, 770 (2000).

[6] S. Fan, P.R. Villeneuve, J.D. Joannopoulos, and E.F. Schubert, Phys. Rev. Lett. **78**, 3294 (1997).

[7] H. Miyazaki and K. Ohtaka, Phys. Rev. B **58**, 6920 (1998).

[8] R. Shimada, Y. Komori, T. Koda, T. Fujimura, T. Itoh, and K. Ohtaka, Mol. Cryst. Liq. Cryst. Sci. Technol., Sect. A **349**, 5 (2000).

[9] T. Yamasaki and T. Tsutsui, Jpn. J. Appl. Phys., Part 1 **38**, 5916 (1999).

[10] H.T. Miyazaki, H. Miyazaki, K. Ohtaka, and T. Sato, J. Appl. Phys. **87**, 7152 (2000).

[11] T. Fujimura, T. Itoh, A. Imada, R. Shimada, T. Koda, N. Chiba, H. Muramatsu, H. Miyazaki, and K. Ohtaka, J. Lumin. **87-89**, 954 (2000).

[12] S. Chu, Science **253**, 861 (1991).

[13] G. Mie, Ann. Phys. (Leipzig) **25**, 377 (1908); M. Born and E. Wolf, *Principles of Optics* (Pergamon, Oxford, 1965), p. 633.

[14] G. Bosi, J. Opt. Soc. Am. B **13**, 1691 (1996).

[15] K. Ohtaka, J. Phys. C **13**, 667 (1980).